

Climate Variability and Child Undernutrition in Cambodia: A Spatial Analysis Using Demographic and Health Survey 2021–2022 and Climate Satellite-Derived Data 2020

Pichsokkim Pav^{1*}, Channarong Phan², Samnang Um², Heng Sopheab²

¹Calmette Hospital, Phnom Penh, Cambodia

² National Institute of Public Health (NIPH), Phnom Penh, Cambodia

*Corresponding author's email: pichsokkimpav@gmail.com

Abstract

Background: While socio-economic determinants of malnutrition are well-documented, the influence of climate variability on regional undernutrition disparities in Cambodia remains under-researched. This study aimed to assess the spatial clustering of child undernutrition in Cambodia and examine its cluster-level ecological associations with hydro-climatic variability and socioeconomic vulnerability using CDHS 2021–2022 data.

Methods: We linked 706 georeferenced cluster locations from the Cambodia Demographic and Health Survey (CDHS) 2021–2022 with high-resolution climate datasets (CHIRPS, MODIS). Spatial autocorrelation was tested using Getis-Ord G_i^* statistics, and generalized linear models (GLMs) were used to quantify the impact of environmental predictors on cluster-level prevalence.

Results: Significant spatial clustering of stunting was identified in the northern and northeastern provinces (Ratanakkiri 39%, Mondulokiri 29%), forming a "Northeast corridor" of chronic vulnerability. Regression analysis identified the Enhanced Vegetation Index (EVI) as the most potent predictor of stunting ($B = 1.33$, $p = 0.014$), highlighting risks in densely forested, remote highland regions. Conversely, annual wet days served as a significant protective factor for underweight ($B = -0.16$, $p = 0.013$). Wasting and underweight were less sensitive to long-term climate variables but showed high spatial heterogeneity, with wasting hotspots peaking in southern and southeastern pockets.

Conclusion: Climate variability, specifically drought frequency and low ecosystem productivity (EVI), are critical ecological drivers of chronic malnutrition in Cambodia. Targeted, climate-sensitive nutrition interventions are required for identified high-risk geographic hotspots, particularly in isolated highland clusters.

Keywords: Child undernutrition, Climate variability, Drought, Cambodia, Spatial analysis

Introduction

Child undernutrition remains a major global health challenge particularly in developing countries. It manifests as stunting (low height-for-age), wasting (low weight-for height), and underweight (low weight-for-age), which defined as a z-score below -2 standard deviations of WHO growth standards [1]. In 2022, an estimated 149 million children under five were affected by stunting, and 45 million by wasting worldwide [2]. Undernutrition contributes to nearly half of all child deaths in developing countries and impairs physical growth, cognitive development, and long-term socioeconomic productivity [3].

In Southeast Asia, approximately 27.4% of children under five live with stunting [4, 5]. According to the CDHS 2021–2022, Cambodia faces a stunting prevalence of 23.2%, wasting at 9.9%, and underweight at 16.4%. While Cambodia has made progress, regional disparities persist, particularly in remote and climate-vulnerable areas [6].

While Cambodia has made progress in reducing these rates over the last decade, regional disparities persist, particularly in remote and climate-vulnerable areas [6]. These levels remain above regional averages and far from national targets, despite the government’s commitment to reducing stunting by 40% and wasting below 5% by 2025, consistent with Sustainable Development Goal (SDG) 2.2 [2, 7].

Furthermore, increasing evidence has shown that climate variability further exacerbates child undernutrition. Changes in rainfall, temperature, vegetation cover, and drought conditions influence agricultural productivity, food availability, and household livelihoods. Extreme events such as floods and prolonged droughts disrupt food systems and increase exposure to infectious diseases. Studies across low and middle-income countries (LMIC), including studies using DHS data, have linked to low rainfall, elevated temperatures, and reduced vegetation density with higher risks of stunting and wasting [8, 9]. However, such climate variability and child nutrition linkages remain understudied in Cambodia.

Although various programs—such as UNICEF’s Integrated Early Childhood Development interventions and the World Food Programme’s nutrition initiatives—aim to address child

undernutrition, few have explicitly incorporated climate-sensitive approaches or integrate environmental data into planning [2, 10]. This represents a critical gap, especially as Cambodia faces recurrent floods, droughts, and increasing climate uncertainty. To address the critical gap in climate-sensitive nutrition research in Cambodia, this study applies a socio-ecological framework to examine the intersection of environmental and socioeconomic characteristics. The study aims to assess the spatial clustering of child undernutrition (stunting, wasting, and underweight) in Cambodia and to examine cluster-level ecological associations between hydro-climatic variability (temperature, rainfall, frequency of wet days, precipitation patterns, drought episodes, aridity, and evapotranspiration), environmental conditions (vegetation index, irrigation coverage, elevation), and socioeconomic and access-related factors (travel time to cities, household poverty, maternal education, and water and sanitation access), using data from the Cambodia Demographic and Health Survey 2021–2022.

Methods

Study Design and Data Integration

This cross-sectional study conducted a secondary analysis of the Cambodia Demographic and Health Survey (CDHS) 2021–2022, which employed a stratified, two-stage cluster sampling design to collect nationally representative data on child health, nutrition, and household characteristics [6]. Georeferenced data were available for 706 clusters across 25 provinces [6]. To ensure confidentiality, GPS coordinates were displaced up to 2 km for urban and 5 km for rural clusters per DHS protocol [6, 11]. Environmental and accessibility covariates were linked to cluster coordinates using standardized raster extraction procedures from the DHS Spatial Data Repository [11].

Child Nutrition Indicators and Data Cleaning

Anthropometric Z-scores were calculated using the WHO Child Growth Standards [1].

- **Nutritional Outcomes:** We defined 1) Stunting (height-for-age), 2) Wasting (weight-for-height), and 3) Underweight (weight-for-age) using a Z-score cutoff of <-2 standard deviations (SD).

- **Data Processing:** Biologically implausible values were excluded according to WHO flagging criteria.
- **Aggregation:** Individual records were then aggregated to the cluster level to calculate the prevalence (proportion) of each indicator, serving as the dependent variables for spatial and statistical modeling.

Geospatial Covariate Extraction and Integration

We linked the 706 clusters to high-resolution, satellite-derived environmental datasets for the year 2020 to capture the antecedent effects of climate variability on nutritional outcomes [11]. Following the DHS Geospatial Covariate framework [11], we extracted data using a spatial buffer approach:

- **Climate and Temperature:** Air temperature variables (mean, maximum, minimum, PET) were obtained from the Climatic Research Unit Time-Series dataset (CRU TS v4.05) [12]. Land Surface Temperature (day and night) was derived from MODIS satellite products produced by NASA [13]. Diurnal temperature range was calculated as the difference between day and night LST [13].
- **Precipitation and Moisture:** Annual rainfall and wet days were extracted from the CHIRPS dataset developed by the Climate Hazards Center [14]. The aridity index was calculated as the ratio of annual precipitation to potential evapotranspiration [12]. Drought frequency was derived from the global hazard dataset published by the World Bank [15].
- **Vegetation and Land Productivity:** Vegetation productivity was measured using the Enhanced Vegetation Index (EVI) derived from the MODIS MOD13 dataset [16].
- **Topography and Agriculture:** Elevation data were obtained from the Shuttle Radar Topography Mission (SRTM) dataset [17]. Irrigated area coverage and growing season length were derived from FAO global agroecological datasets [18].
- **Accessibility and Human Influence:** Travel time to the nearest high-density urban center was obtained from the global accessibility surface developed by the Malaria Atlas Project [19]. Human land modification was measured using the Global Human Footprint dataset developed by the Wildlife Conservation Society and CIESIN [20]. Nighttime light intensity was derived from satellite-based observations provided by the National Oceanic and Atmospheric Administration [21].

All geospatial variables were aggregated to the cluster level for integration with socioeconomic and health indicators.

Socioeconomic and Health Covariates

Socioeconomic status was derived from the Cambodia Demographic and Health Survey (CDHS) 2021–2022 dataset [6]. Specifically, cluster-level proportions of households classified as poor, of mothers with no schooling or informal education, and of households with access to improved water and sanitation (WASH) facilities. In addition, childhood morbidity indicators were constructed by estimating the cluster-level prevalence of fever and diarrhea reported among children in the two weeks preceding the survey.

Statistical Methods

Descriptive Analysis

Initially, we calculated cluster-level means, standard deviations, and ranges for all 706 georeferenced clusters. To prepare for modeling, the cluster-level prevalence of stunting, wasting, and underweight was log-transformed to achieve a normal distribution and stabilize variance.

Spatial Autocorrelation and Hotspot Analysis

Spatial patterns of undernutrition were examined using Getis-Ord G_i^* statistics to identify statistically significant hotspots and coldspots. A fixed-distance band (38 km) was applied to ensure adequate spatial connectivity across all clusters. Visualizations and spatial processing were conducted in R (version 4.x) using the *sf* and *tmap* packages [22-24].

Statistical Modeling

Cluster-level prevalence of undernutrition outcomes was log-transformed for normality. Multivariable linear regression models were used to quantify associations between environmental and socioeconomic predictors and nutritional outcomes. Models were fitted in two stages:

- 1) Unadjusted models assessing raw associations between predictors and outcomes.

- 2) Adjusted models controlling for socioeconomic confounders, including household poverty, maternal education, and cluster-level access to improved water and sanitation.

All statistical analyses were conducted in Stata 18, and significance was defined at $p < 0.05$.

Ethical Considerations

This study constitutes a secondary analysis of de-identified data from the Cambodia Demographic and Health Survey (CDHS) 2021–2022. Access to the raw datasets was granted by the DHS Program following the approval of a research registration. The original survey protocol received ethical clearance from the Cambodia National Ethics Committee for Health Research (NECHR, Ref #83, dated May 10, 2021) and the Institutional Review Board (IRB) of ICF in Rockville, MD, USA. During the primary data collection, written informed consent was obtained from all adult participants and from parents or guardians for children under the age of 18. Cluster-level environmental and climate covariates were obtained from the DHS Spatial Data Repository (<https://spatialdata.dhsprogram.com/covariates/>).

Results

Spatial Distribution of Undernutrition

At the national level, the prevalence of stunting is 21.5%, wasting is 9.9%, and underweight is 16.4%, though these figures mask significant regional heterogeneity. Stunting—indicative of chronic malnutrition—is most severe in the Northeast plateau provinces of Ratanakkiri (39%) and Mondulkiri (29%), as visually evidenced by the high-density red clusters in those regions (**Fig 1A**). While acute malnutrition (wasting) shows a different spatial logic, peaking in Kampong Chhnang (31%), it appears more geographically dispersed across the central lowland plains (**Fig 1B**).

Cluster-level analysis further exposes this marked geographic variation; the mean prevalence of stunting across survey clusters is 23.2% (SD: 22.9), ranging from 0% to 100% in the most burdened areas (**Table 1**). Underweight prevalence (mean 16.4%, SD: 18.9) closely mirrors these chronic patterns, with the highest burden consistently appearing in the North and Northeast (**Fig 1C**). While chronic undernutrition is widespread, acute wasting is more geographically concentrated; over 60.8% of clusters reported zero cases of wasting, whereas approximately 9% of clusters exhibited a high stunting burden exceeding 50%.

Morbidity and Socio-Health Characteristics

Nutritional outcomes are closely intertwined with morbidity and socioeconomic barriers. Fever and diarrhea affect an average of 13.8% (SD: 18.8) and 6.3% (SD: 12.9) of children per cluster, respectively (**Table 1**). The spatial correlation is particularly visible in northern regions, where high fever rates (**Fig 1D**) and diarrhea prevalence (**Fig 1E**) overlap with identified malnutrition clusters.

Structural drivers of these disparities are evident in the socioeconomic data: the mean percentage of households classified as poor per cluster is 46.4% (SD: 38.4), and the prevalence of low maternal education averages 42.3% (SD: 30.4) (**Table 1**). Notably, in 20.3% of clusters, every surveyed household was classified as poor, highlighting pockets of extreme vulnerability.

Although national access to improved drinking water (81.4%) and sanitation (83.6%) is relatively high, the spatial overlap between environmental stressors and malnutrition in the Northeast suggests that remaining gaps in infrastructure are primary drivers of regional health disparities. These patterns confirm a "Northeast corridor" of vulnerability where high poverty, low education, and environmental stressors converge.

Climate and Environmental Characteristics

Key climate and environmental characteristics across the 706 survey clusters are summarized in **Table 1**. The average growing season lasted 10.2 months (SD: 0.7), while only 6.9% (SD: 9.9) of cluster areas were irrigated. Elevation varied significantly, ranging from 2.1 to 813.7 meters (mean 57.9 m). Thermal conditions showed daytime land surface temperatures averaging 32.86°C and nighttime temperatures averaging 23.96°C, resulting in a mean diurnal range of 8.7°C. Annual precipitation averaged 1,813.9 mm (SD: 502.8), with an average of 3.8 drought episodes per year. Mean travel time to the nearest city was 100 minutes (SD: 84.1), reflecting notable spatial isolation in certain regions that may influence child health outcomes.

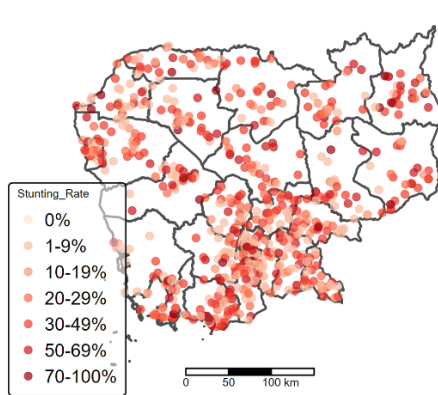
Table 1. Cluster-Level Climate, Environmental, and Child Nutrition Characteristics (N=706 clusters)

Variables	Mean	SD	Min	Max
Climate and Environmental				
Aridity Index	40.7	9.7	29.6	79.8
Land Surface Temp (°C)	28.4	1.1	23.6	30.5
Day LST (°C)	32.9	1.7	26.6	36.4
Night LST (°C)	24.0	0.9	18.7	25.5
Diurnal Temp Range (°C)	8.7	0.6	7.8	10.3
Max Temp (°C)	32.6	0.7	29.9	34.1
Min Temp (°C)	23.9	0.5	21.3	24.5
Mean Temp (°C)	28.2	0.6	25.6	29.0
Drought Episodes (count)	3.8	3.2	0.0	8.0
Elevation (m)	58.6	89.5	2.1	813.7
Enhanced Vegetation Index (EVI)	0.3	0.1	0.2	0.6

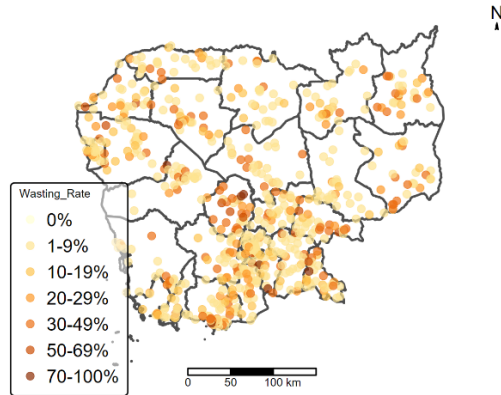
Potential Evapotranspiration (PET)	3.8	0.2	3.3	4.1
Annual Precipitation (mm/month)	153	31	108	269
Annual Rainfall (mm)	1814	503	1553	3664
Wet Days (count)	11.0	1.2	9.5	14.2
Global Human Footprint	35.8	11.8	0.0	75.7
Nightlights Composite	0.5	2.4	0.0	21.1
Irrigated Area (%)	6.8	9.9	0.0	70.4
Growing Season Length (months)	10.2	0.7	9.0	12.0
Socioeconomic				
Household Poverty (%)	46.4	38.4	0.0	100.0
Low Maternal Education (%)	42.3	30.4	0.0	100.0
Travel Time to City (minutes)	101	84	0	519
Improved Water Access (%)	81.4	28.1	0.0	100.0
Improved Toilet Access (%)	83.6	25.4	0.0	100.0
U5 Population (per cluster)	1340	3809	2	32148
Nutrition and Health				
Stunted (%)	23.2	22.9	0.0	100.0
Wasted (%)	9.9	15.4	0.0	100.0
Underweight (%)	16.4	18.9	0.0	100.0
Fever (%)	13.8	18.8	0.0	100.0
Diarrhea (%)	6.3	12.9	0.0	100.0

Data Source: Compiled from the Cambodia Demographic and Health Survey (CDHS) 2021–2022 and high-resolution climate datasets (CHIRPS, MODIS) for the year 2020. **Notes:** Values represent cluster-level means across 706 georeferenced enumeration areas. **Abbreviations:** EVI: Enhanced Vegetation Index; LST: Land Surface Temperature; PET: Potential Evapotranspiration; U5: Children Under Five Years Old; SD: Standard Deviation.

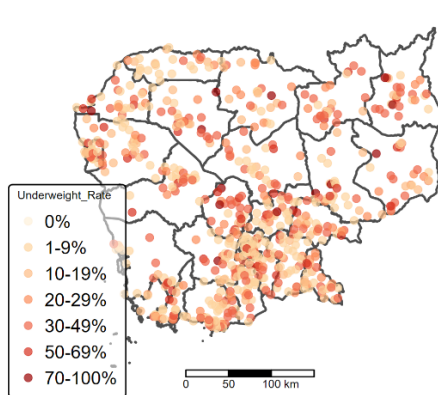
A. Stunting Prevalence



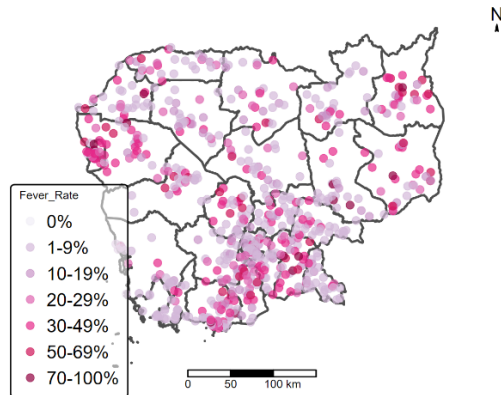
B. Wasting Prevalence



C. Underweight Prevalence



D. Fever Prevalence



E. Diarrhea Prevalence

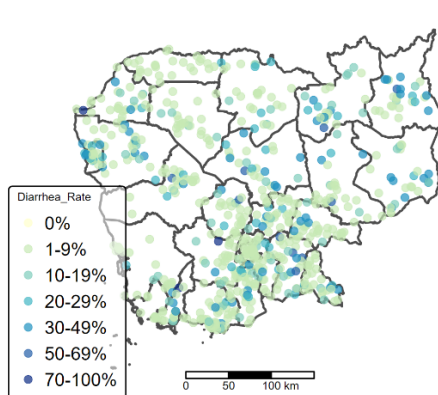
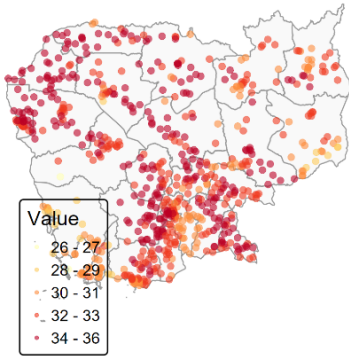
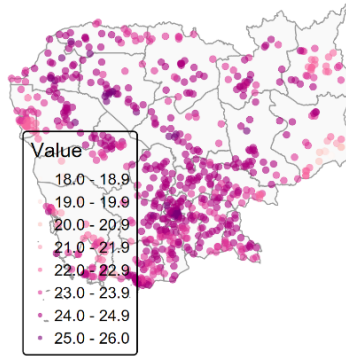


Figure 1. Cluster-Level Distribution of Stunting, Wasting, Underweight, Fever, and Diarrhea Among Children Under Five in Cambodia, 2021–2022.

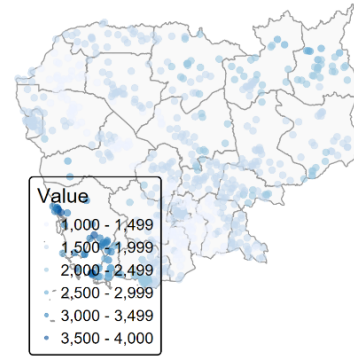
A. Day Temp (°C)



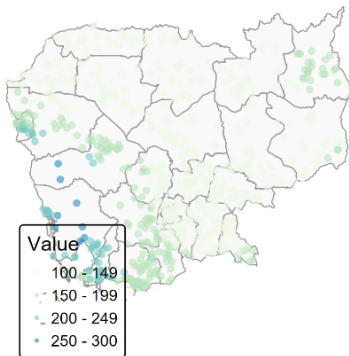
B. Night Temp (°C)



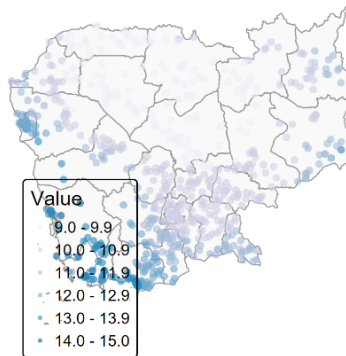
C. Annual Rainfall



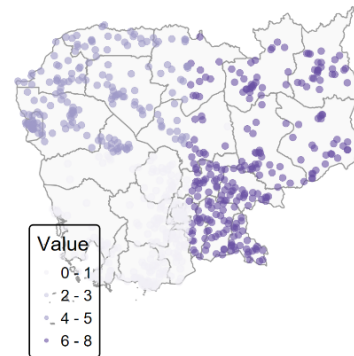
D. Avg Precipitation



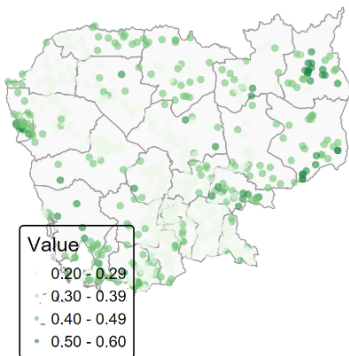
E. Wet Days Count



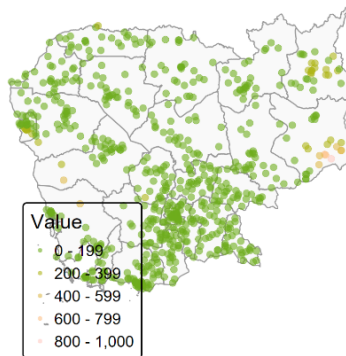
F. Drought Frequency



G. Vegetation (EVI)



H. Elevation (m)



I. Urban Access (min)

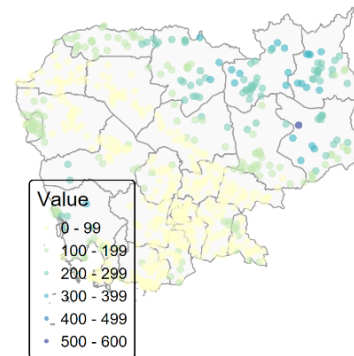


Figure 2. Spatial Distribution of Climate and Environmental Predictors across Survey Clusters, including Vegetation Index (EVI), Surface Temperature, and Drought Frequency.

Spatial Hot Spot Analysis of Undernutrition (Getis-Ord G_i^*)

The hotspot analysis identifies statistically significant spatial clusters where the prevalence of undernutrition is higher (**Hotspots**) or lower (**Coldspots**) than the national average. Significant geographic clustering was observed for all three indicators (**Fig 3**), utilizing a fixed-distance band of 38,063 meters to ensure rigorous spatial connectivity across all 706 clusters. This methodological approach confirms that undernutrition in Cambodia is not a uniform burden but a collection of distinct "geographies of hunger" that transcend provincial borders.

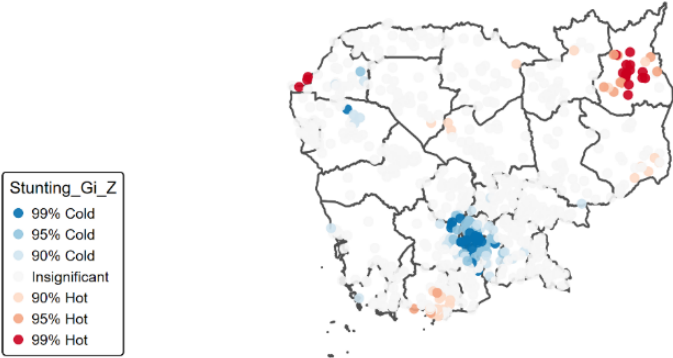
Stunting hotspots (**Map A**) are concentrated primarily in the Northeast and Eastern clusters, identifying a "Northeast corridor" of chronic undernutrition. The most intense hotspots (99% confidence, red) are anchored in the highland provinces of Ratanakkiri and Monduliri, with maximum Z-scores reaching 4.62. This confirms that stunting is a regional structural crisis in the highlands rather than an isolated provincial issue. Because stunting measures linear growth retardation over time, its concentration in these specific regions suggests persistent, systemic drivers such as geographic isolation, limited market access, and long-term nutritional deficits.

In contrast, wasting hotspots (**Map B**) exhibit a completely different spatial signature characterized by intense spatial polarization. While the Central Plains emerge as significant coldspots (95–99% confidence, blue), pronounced hotspots are found in the South and Southeast. Wasting Z-scores reached a study-high of 6.51 (e.g., Cluster 108), indicating the most statistically significant clustering in the dataset. Notably, several clusters with 0% wasting were flagged as significant hotspots due to their proximity to high-prevalence neighbors. This "neighborhood effect" suggests a regional susceptibility to acute shocks, where children in the southern coastal or border areas are significantly less protected from acute weight loss compared to those in the central "breadbasket" regions.

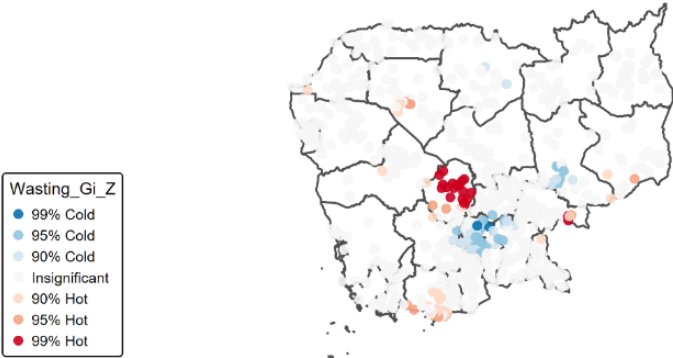
Underweight hotspots (**Map C**) appear as a more fragmented composite indicator. These clusters show some spatial overlap with the Northern stunting corridor but feature fewer areas reaching high statistical significance. The more dispersed nature of underweight clustering suggests it is influenced by a complex mixture of both chronic and acute factors, lacking the singular geographic intensity seen in the stunting highlands or the wasting lowlands. These findings collectively

highlight the need for dual-track interventions: long-term structural support for the chronic "Northeast corridor" and rapid-response nutritional monitoring for the acute "Southern pockets."

A. Stunting Hotspots



B. Wasting Hotspots



C. Underweight Hotspots

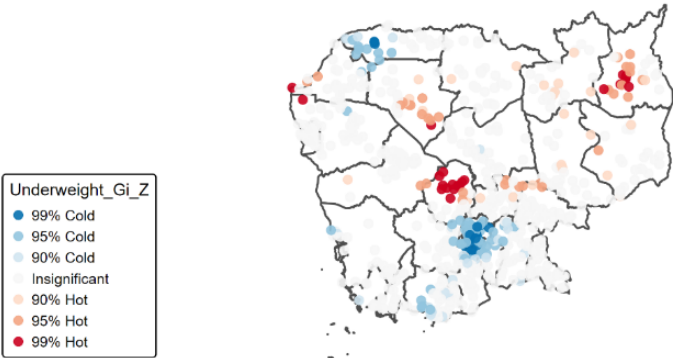


Figure 3. Spatial Hot Spot Analysis (**Getis-Ord Gi***) of Child Undernutrition. Red areas indicate statistically significant hotspots ($p < 0.05$) using a fixed-distance spatial weight matrix of 38,063 meters.

Unadjusted Associations with Environmental and Socioeconomic Predictors

Unadjusted linear regression models at the cluster level identified several significant environmental and socioeconomic predictors of child undernutrition. These factors are categorized into socioeconomic drivers and climate-related environmental determinants.

Household poverty and low maternal education were the most consistent predictors of nutritional deficits. Both factors showed strong positive associations with stunting (Coeff = 0.356 and 0.438, $p < 0.001$), wasting (Coeff = 0.166, $p < 0.01$; Coeff = 0.246, $p < 0.010$), and underweight (Coeff = 0.447 and 0.486, $p < 0.001$). Access to improved water (Coeff = -0.348, $p < 0.001$) and improved toilets (Coeff = -0.360, $p < 0.001$) were significantly associated with lower stunting and underweight prevalence. Travel time to the nearest city was positively associated with stunting (Coeff = 0.002, $p < 0.001$) and underweight (Coeff = 0.001, $p < 0.001$), indicating that geographic isolation increases malnutrition risk. Annual drought episodes were significantly associated with a higher log-prevalence of stunting (Coeff = 0.024, $p < 0.010$) and underweight (Coeff = 0.024, $p < 0.010$). Conversely, a higher number of annual wet days was protective against underweight status (Coeff = -0.048, $p < 0.05$). The Enhanced Vegetation Index (EVI) showed a strong positive association with stunting (Coeff = 1.752, $p < 0.001$) and underweight (Coeff = 1.311, $p < 0.001$). Elevation was positively associated with stunting (Coeff = 0.001, $p < 0.001$) and underweight (Coeff = 0.001, $p < 0.010$), while irrigation coverage served as a protective factor specifically against stunting (Coeff = -0.007, $p < 0.010$). Additionally, mean temperature exhibited a significant negative association with stunting (Coeff = -0.210, $p < 0.001$) and underweight (Coeff = -0.120, $p < 0.05$).

Table 2. Unadjusted Associations between Environmental/Socioeconomic Predictors and Child Undernutrition (Log-Prevalence)

Predictors	Stunting (Log)	Wasting (Log)	Underweight (Log)
	Coeff (Std. Err.)	Coeff (Std. Err.)	Coeff (Std. Err.)
Socioeconomic			
Travel Time to City (min)	0.002 (0.000)***	0.000 (0.000)	0.001 (0.000)***
Household Poverty (%)	0.356 (0.072)***	0.166 (0.061)**	0.447 (0.066)***
Maternal Low Education (%)	0.438 (0.092)***	0.246 (0.077)**	0.486 (0.085)***
Improved Water Access (%)	-0.348 (0.100)***	-0.113 (0.084)	-0.323 (0.093)***
Improved Toilet Access (%)	-0.360 (0.110)***	-0.127 (0.093)	-0.464 (0.102)***
Climate and Environmental			

Day Temperature (LST) (°C)	-0.011 (0.017)	-0.005 (0.014)	-0.004 (0.016)
Diurnal Temp Range (°C)	0.019 (0.049)	-0.007 (0.041)	0.037 (0.046)
Mean Temperature (°C)	-0.210 (0.051)***	-0.070 (0.043)	-0.120 (0.048)*
Aridity Index	-0.000 (0.003)	0.001 (0.002)	-0.001 (0.003)
Potential Evapotranspiration (PET)	-0.314 (0.159)*	-0.147 (0.133)	-0.139 (0.148)
Annual Rainfall (mm)	0.000 (0.000)	0.000 (0.000)	0.000 (0.000)
Annual Precipitation (mm/month)	-0.000 (0.001)	0.000 (0.001)	-0.001 (0.001)
Annual Wet Days (count)	-0.019 (0.024)	0.010 (0.020)	-0.048 (0.022)*
Drought Episodes (count)	0.024 (0.009)**	-0.007 (0.007)	0.024 (0.008)**
Enhanced Vegetation Index (EVI)	1.752 (0.392)***	0.550 (0.331)	1.311 (0.367)***
Irrigation Coverage	-0.007 (0.003)**	0.000 (0.002)	-0.002 (0.003)
Elevation (m)	0.001 (0.000)***	0.000 (0.000)	0.001 (0.000)**

Statistical Note: *Coeff* (Coefficient) represents the estimated change in the log-prevalence of the outcome for every unit increase in the predictor. **Std. Err.** (Standard Error) indicates the precision of the estimate. **Significance:** Statistical significance is denoted by stars: *** $p < 0.001$, ** $p < 0.01$, * $p < 0.05$. **Sample Size:** N ranges from 694 to 698 clusters due to missing GPS or covariate data in specific locations.

Determinants of Child Undernutrition

The multiple linear regression models (**Table 3**) identify the environmental and socioeconomic drivers of undernutrition across 706 clusters.

Determinants of Stunting (Chronic Malnutrition)

The regression model for stunting (Adjusted $R^2 = 0.065$, $p < 0.001$) indicates that chronic undernutrition in Cambodia is primarily a structural and geographic issue. The most potent predictor was the Enhanced Vegetation Index (EVI) (Coeff = 1.33, $p = 0.014$), suggesting that stunting is heavily concentrated in the densely forested, remote highland regions. This is further compounded by low maternal education (Coeff = 0.27, $p = 0.009$), which acts as a critical socio-structural barrier. Notably, immediate climatic factors like rainfall and temperature did not reach statistical significance. This confirms that stunting is the result of long-term, persistent challenges—such as geographic isolation from food markets and healthcare—rather than seasonal weather fluctuations.

Determinants of Wasting (Acute Malnutrition)

The wasting model (Adjusted $R^2 = 0.011$, $p = 0.092$) reflects the volatile and shock-sensitive nature of acute weight loss. Unlike the structural drivers of stunting, wasting was primarily predicted by household poverty (Coeff = 0.17, $p = 0.053$) and low maternal education (Coeff = 0.18, $p = 0.049$). Furthermore, drought episodes emerged as a near-significant predictor ($p = 0.064$). This indicates that wasting in the southern lowlands is triggered by acute shocks, where climatically vulnerable households, already weakened by poverty, are unable to buffer the nutritional impact of a drought or a failed harvest.

Determinants of Underweight (Composite Malnutrition)

The underweight model provided the strongest statistical fit (Adjusted $R^2 = 0.074$, $p < 0.001$), capturing a "double burden" of risk factors. It was significantly driven by the intersection of poverty (Coeff = 0.24, $p = 0.011$) and low maternal education (Coeff = 0.31, $p = 0.002$). Environmentally, the number of annual wet days served as a significant protective factor (Coeff =

-0.16, $p = 0.013$), suggesting that consistent precipitation stabilizes local food security. This model bridges the previous findings, showing that underweight status serves as a composite indicator influenced by both the long-term structural neglect found in stunting hotspots and the acute environmental instability found in wasting pockets.

Table 3. Determinants of Child Undernutrition: Cluster-Level Multiple Linear Regression Results

Predictors	Stunting (Log)	Wasting (Log)	Underweight (Log)
	Coeff (Std. Err.)	Coeff (Std. Err.)	Coeff (Std. Err.)
Socioeconomic			
Household Poverty (%)	0.158 (0.104)	0.174* (0.089)	0.246** (0.096)
Maternal Low Education (%)	0.273*** (0.105)	0.177** (0.090)	0.310*** (0.097)
Travel Time to City (min)	0.001 (0.001)	-0.001 (0.001)	0.001 (0.001)
Improved Water Access (%)	-0.095 (0.118)	0.019 (0.101)	-0.003 (0.109)
Improved Toilet Access (%)	0.188 (0.141)	0.092 (0.120)	-0.015 (0.130)
Climate and Environmental			
Annual Wet Days (count)	-0.019 (0.073)	0.018 (0.063)	-0.169** (0.068)
Drought Episodes (count)	-0.011 (0.013)	-0.021* (0.011)	-0.001 (0.012)
Vegetation Index (EVI)	1.334** (0.543)	0.670 (0.466)	0.702 (0.504)
Day Temperature (LST)	0.016 (0.021)	0.001 (0.018)	0.001 (0.019)
Elevation (m)	-0.001 (0.001)	-0.001 (0.001)	0.001 (0.001)
Intercept			
Constant	8.294** (4.069)	5.028 (3.488)	1.714 (3.769)
Model Diagnostics			
Observations (N)	694	694	695
R-squared	0.088	0.036	0.097
Adjusted R-squared	0.065	0.011	0.074
Prob > F	0.0000	0.0929	0.0000

Statistical Note: Results are based on Cluster-Level Multiple Linear Regression.

Adjustments: Models include adjustments for socio-economic factors and environmental covariates.

Significance Levels: * $p < 0.10$, ** $p < 0.05$, *** $p < 0.01$.

Model Diagnostics: Reported Adjusted R-squared values indicate the proportion of variance explained by the model (Stunting: 0.065; Wasting: 0.011; Underweight: 0.074).

Abbreviations: Coeff: Coefficient; SE: Standard Error; EVI: Enhanced Vegetation Index; LST: Land Surface Temperature.

Discussion

This study provides a high-resolution ecological analysis of the environmental and climatic determinants of child undernutrition in Cambodia. By linking CDHS 2021–2022 anthropometric data with satellite-derived hydro-climatic layers from 2020, we identified distinct "*geographies of hunger*" that reveal how landscape-level constraints and climate variability exacerbate structural socioeconomic vulnerabilities. Our findings align with global evidence from other low- and middle-income countries (LMICs) regarding the climate-health nexus, while highlighting regional paradoxes unique to the Mekong sub-region [1, 25-27].

A central finding was the identification of a statistically significant hotspot of chronic undernutrition in Cambodia's northeastern provinces. In the global LMIC context, higher vegetation indices are typically associated with improved nutritional outcomes due to increased agricultural productivity and food availability [28-30]. However, our results demonstrate an EVI in Cambodia, where a higher EVI was the strongest predictor of stunting (Coeff = 1.334, $p < 0.05$). From an epidemiological perspective, high EVI in the Cambodian highlands serves as an ecological proxy for dense primary forest and rugged topography rather than productive cropland. This represents a form of geographic marginalization common in mountainous LMIC regions [31, 32]. Families in these high-EVI clusters face extreme spatial isolation, with mean travel times to urban centers exceeding 100 minutes [33]. This physical distance limits access to diverse food markets and to the Ministry of Health's decentralized services. For these populations, the landscape itself acts as a distal driver of linear growth failure [26, 27].

In contrast to the structural nature of stunting, wasting (weight-for-height) exhibited a volatile spatial signature peaking in the southern plains. Globally, wasting in LMICs is increasingly linked to extreme weather events that disrupt immediate food access [25, 34]. Our identification of drought episodes as a critical trigger for wasting ($p = 0.064$) underscores a major public health vulnerability. In Cambodia's southern "breadbasket," irrigation coverage is strikingly low (6.9%). Consequently, households rely almost exclusively on rain-fed rice monoculture. A single failed monsoon translates directly into a biological shock for children, as households lack the agro-

ecological buffers—such as water storage or diversified livelihoods—to mitigate the impact of a failed harvest [35, 36].

Underweight status (weight-for-age) served as our most robust composite indicator, reflecting both chronic and acute stress. A key finding was the protective role of annual wet days (Coeff = -0.169, $p < 0.05$). In rural Cambodia, as in many LMICs, nutritional stability is often maintained through "homestead food production"—small-scale gardening and poultry raising. These activities are highly dependent on the consistency of the rainy season rather than the total volume of precipitation [34, 35]. Predictable wet days ensure a steady supply of micronutrients and animal-source proteins. As climate change increases rainfall variability, this vital nutritional "safety net" is eroded.

Consistent with the UNICEF Conceptual Framework, socioeconomic factors remained fundamental. Low maternal education was a universal risk factor across all nutritional phenotypes ($p < 0.01$) [1, 6]. Maternal education acts as the primary mediator of climate risk. Educated mothers are more likely to utilize WASH (Water, Sanitation, and Hygiene) facilities correctly and seek healthcare during climate-induced "lean seasons." The spatial overlap we observed between fever/diarrhea clusters and malnutrition hotspots confirms a synergistic "malnutrition-infection" cycle where climate-driven water scarcity exacerbates water-borne pathogens, further impairing nutrient absorption [26, 37].

Policy Implications

Our findings suggest that the Royal Government of Cambodia's goal to reduce stunting to 19% and wasting below 5% by 2030 (SDG 2.2.2) requires a transition from general nutritional support to climate-sensitive, geographically targeted interventions [7].

Short-term: Rapid Response and Surveillance

The Ministry of Health must integrate satellite-derived hydro-climatic data into existing community nutrition surveillance. Establishing an Early Warning, Early Action (EWEA) system can trigger the distribution of therapeutic foods and micronutrients before climate shocks manifest

as clinical wasting. Immediate mobile health outreach should be prioritized for high-EVI "Northeast corridor" clusters to bypass physical travel barriers.

Medium-term: Building Sub-National Resilience

Policy must shift toward strengthening infrastructure to buffer against environmental volatility. As maternal education is a universal protective factor ($p < 0.01$), the government should scale up culturally tailored, climate-smart Social and Behavior Change Communication (SBCC) programs. Simultaneously, increasing irrigation coverage is critical to stabilize the "wet days" effect, allowing households to maintain food production regardless of monsoon shifts.

Long-term: Structural and Multi-Sectoral Adaptation

Long-term transformation requires the structural integration of the National Strategy for Food Security and Nutrition with the National Climate Change Action Plan for Public Health, 2020-204, and the current consultative framework for 2025–2030 [38]. Efforts must focus on reducing the geographic marginalization of the northeast plateau through improved rural infrastructure and the promotion of diversified, climate-resilient livelihoods that reduce reliance on forest-based subsistence.

Strengths and Limitations

A major strength of this study is the integration of cluster-level DHS data with antecedent climate layers (2020), capturing the delayed effects of environmental stress on child growth. However, the cross-sectional design precludes the establishment of direct causality. Additionally, while standard, the 2–5 km GPS displacement in DHS data may introduce minor "edge effects" in high-resolution spatial modeling. Future research should utilize longitudinal data to further parse the temporal relationship between specific drought phases and acute weight loss.

Conclusion

In conclusion, child stunting in Cambodia is shaped by both socioeconomic and environmental factors, with climate variability amplifying risks in vulnerable regions. Policymakers should prioritize geographically targeted interventions that integrate nutrition, climate resilience, and

equitable access to services. Strengthening maternal education, promoting household food security, and implementing climate-adaptive agricultural strategies are likely to yield substantial improvements in child growth outcomes.

Author Contributions

Pichsokkim Pav: Conceptualization; Methodology; Writing – Original Draft; Writing – Review & Editing.

Channnarong Phan: Conceptualization; Project Administration; Writing – Original Draft; Writing – Review & Editing.

Samnang Um: Conceptualization; Resources; Methodology; Validation; Formal Analysis; Investigation; Writing – Review & Editing.

Heng Sopheab: Supervision; Validation; Writing – Review & Editing. All authors (P Pav, C Phan, S Um, H Sopheab) participated in the critical review and editing of the final manuscript

Acknowledgments

We acknowledge the DHS Program and the Spatial Data Repository for data access.

Funding

This study was supported by the Australian Government through a small research grant from Australia Awards Cambodia Round 5. The funder had no role in the study design, data collection and analysis, decision to publish, or preparation of the manuscript. The opinions expressed in this research are those of the authors and do not necessarily reflect the views of the Australian Government or Australia Awards Cambodia.

Data Availability Statement

This study utilizes the 2021–2022 Cambodia Demographic and Health Survey (CDHS) datasets. The DHS data are publicly available through the DHS Program website (URL: <https://www.dhsprogram.com/data/available-datasets.cfm>). Geospatial covariate data were obtained from the Spatial Data Repository (URL: <https://spatialdata.dhsprogram.com/covariates/>). Shapefiles for administrative boundaries in Cambodia are publicly accessible via the DHS spatial data portal (URL: <https://spatialdata.dhsprogram.com/boundaries/#view=table&countryId=KH>).

Conflicts of Interest

The authors have declared that no competing interests exist.

Abbreviations

WHO: World Health Organization; **CDHS:** Cambodia Demographic and Health Survey; **GPS:** Global Positioning System coordinates; **EVI:** Enhanced Vegetation Index; **NDVI:** Normalized Difference Vegetation Index; **LST:** Land Surface Temperature; **CHIRPS:** Climate Hazards Group InfraRed Precipitation with Station data; **SPI:** Standardized Precipitation Index; **PET:** Potential Evapotranspiration; **GLMs:** Generalized Linear Models; **Gi*:** Getis-Ord Gi*; **GHF:** Global Human Footprint index.

References

1. World Health Organization. The WHO Child Growth Standards. Available from: <https://www.who.int/tools/child-growth-standards/standards>.
2. Cambodia U. Nutrition in Cambodia. 2023.
3. Unicef, Who, World B. Levels and trends in child malnutrition: Joint child malnutrition estimates. Geneva: WHO; 2021.
4. World Health O. Nutrition in the South-East Asia Region. 2023.
5. Global Nutrition R. South-eastern Asia nutrition profile. 2022.
6. National Institute of S. Cambodia Demographic and Health Survey 2021–22: Final Report. Phnom Penh: Ministry of Planning, Cambodia; 2022.
7. National Nutrition Programme NM, Child Health C. Fast Track Road Map for Improving Nutrition 2023–2030. Phnom Penh: Ministry of Health, Royal Government of Cambodia, 2024.
8. Dasgupta S. Climate, weather and child health in Burkina Faso. *Health Economics*. 2022;31(6):753-68. doi: 10.1111/1467-8489.12530.
9. Grace K. Measuring the environmental context of child growth in Burkina Faso. *Environmental Health Perspectives*. 2024;132(5):057001. doi: 10.1289/EHP10745.
10. World Food P. Cambodia. 2023.
11. Mayala B, Donohue R. The DHS Program Geospatial Covariate Datasets Manual (Third Edition). Rockville, Maryland, USA: ICF, 2022 2022. Report No.
12. Harris I, Osborn TJ, Jones P, Lister D. Version 4 of the CRU TS monthly high-resolution gridded multivariate climate dataset. *Sci Data*. 2020;7(1):109. Epub 20200403. doi: 10.1038/s41597-020-0453-3. PubMed PMID: 32246091; PubMed Central PMCID: PMC7125108.
13. Nasa. MODIS Land Surface Temperature and Emissivity (MOD11A1) V6.1. 2021.
14. Chg. CHIRPS pentad: Rainfall estimates from rain gauge and satellite observations. 2021.
15. Huan Wu. Global Flood Monitoring System (GFMS) at ESSIC, University of Maryland Available from: <https://floodobservatory.colorado.edu/Events/4795/2019Cambodia4795.html>.
16. Didan K. MOD13 Vegetation Index Product (EVI). NASA; 2016.
17. Farr TG. The Shuttle Radar Topography Mission. *Reviews of Geophysics*. 2007;45(2):RG2004. doi: 10.1029/2005RG000183.
18. Fao. Global Agro-Ecological Zones (GAEZ v4). Rome: Food and Agriculture Organization, 2021.
19. Weiss DJ, Nelson A, Gibson HS. A global map of travel time to cities in 2015. *Nature*. 2018;553:333-6. doi: 10.1038/nature25181.
20. Wildlife Conservation S, Ciesin. Global Human Footprint Dataset. New York: Columbia University; 2005.

21. Information NNCfE. VIIRS Nighttime Lights Data. 2020.
22. Team RC. R: A Language and Environment for Statistical Computing. Vienna, Austria: R Foundation for Statistical Computing; 2023.
23. Pebesma E. Simple Features for R: Standardized Support for Spatial Vector Data. *The R Journal*. 2018;10(1):439-46. doi: 10.32146/journal.01.2018.1.
24. Tennekes M. tmap: Thematic Maps in R. *Journal of Statistical Software*. 2018;84(6):1-39. doi: 10.18637/jss.v084.i06.
25. Unicef, Who, World Bank G. Joint Child Malnutrition Estimates: Levels and trends in child malnutrition: Key findings of the 2023 edition. 2023.
26. Black RE, Victora CG, Walker SP, Bhutta ZA, Christian P, de Onis M, et al. Maternal and child undernutrition and overweight in low-income and middle-income countries. *The Lancet*. 2013;382(9890):427-51.
27. Ifpri. Climate change and nutrition in Cambodia: Vulnerability and adaptation strategies. Phnom Penh: IFPRI, 2019.
28. Cooper MW, Brown ME, Hochrainer-Stigler S, Pflug G, McCallum I, Fritz S, et al. Mapping the effects of drought on child stunting. *Proceedings of the National Academy of Sciences USA*. 2019;116(35):17219-24.
29. Didan K. MOD13 Vegetation Index Product (EVI). NASA; 2016.
30. Grace D, Roesel K. Climate change and livestock production in developing countries. *Revue Scientifique et Technique (International Office of Epizootics)*. 2015;34(1):1-13.
31. Akombi BJ, Agho KE, Hall JJ, Wali N, Renzaho AM, Merom D. Stunting, wasting and underweight in sub-Saharan Africa: A systematic review. *International Journal of Environmental Research and Public Health*. 2017;14(8):863.
32. Dilley M, Chen RS, Deichmann U, Lerner-Lam AL, Arnold M. Natural Disaster Hotspots: A Global Risk Analysis. Washington, DC: World Bank, 2005.
33. Weiss DJ, Nelson A, Gibson HS, Temperley W, Peedell S, Lieber A, et al. A global map of travel time to cities in 2015. *Nature*. 2018;553(7688):333-6.
34. Brown ME, Funk CC. Food security under climate change. *Science*. 2008;319(5863):580-1.
35. Mekong River C. State of the Basin Report 2023. Vientiane: MRC Secretariat, 2023.
36. Fao. Global Agro-Ecological Zones (GAEZ v4). Rome: FAO; 2021.
37. Lloyd SJ, Kovats RS, Chalabi Z. Climate change, crop yields, and undernutrition: Development of a model to quantify the impact of climate change on child undernutrition. *Environmental Health Perspectives*. 2011;119(12):1817-23.
38. Health. Mo. National Climate Change Action Plan for Public Health 2025–2030. In: Medicine P, editor. Phnom Penh, Cambodia: National Institute of Public Health; 2025.